
Domain-decomposed Fully Coupled Implicit Methods for a Magnetohydrodynamics Problem*

Serguei Ovtchinnikov¹, Florin Dobrian², Xiao-Chuan Cai³, David Keyes⁴

¹ University of Colorado at Boulder, Department of Computer Science, 430 UCB, Boulder, CO 80309, USA, serguei.ovtchinnikov@colorado.edu

² Old Dominion University, Department of Computer Science, 3300 ECS Building, Norfolk, VA 23529, USA, dobrian@cs.odu.edu

³ University of Colorado at Boulder, Department of Computer Science, 430 UCB, Boulder, CO 80309, USA, cai@cs.colorado.edu

⁴ Columbia University, Department of Applied Physics & Applied Mathematics, 500 W. 120th St., New York, NY 10027, USA, david.keyes@columbia.edu

Summary. We present a parallel fully coupled implicit Newton-Krylov-Schwarz algorithm for the numerical solution of the unsteady magnetic reconnection problem described by a system of reduced magnetohydrodynamics equations in two dimensions. In particular, we discuss the linear and nonlinear convergence, the parallel performance of a third-order implicit algorithm and compare to solutions obtained with an explicit method.

1 Introduction

In the magnetohydrodynamics (MHD) formalism plasma is treated as a conducting fluid satisfying the Navier-Stokes equations coupled with Maxwell's equations [6]. The behavior of an MHD system is complex since it admits phenomena such as Alfvén waves and their instabilities. One of the intrinsic features of MHD is the formation of a singular current density sheet, which is linked to the reconnection of magnetic field lines [3, 9, 10, 12], which in turn leads to the release of energy stored in the magnetic field. Numerical simulation of the reconnection plays an important role in our understanding of physical systems ranging from the solar corona to laboratory fusion devices. Capturing the change of the magnetic field topology requires a more general model than ideal MHD. A resistive Hall MHD system is considered in this paper. To simulate this multi-scale, multi-physics phenomenon, a robust

* The work was partially supported by DOE DE-FC02-01ER25479, DEFC02-04ER25595, NSF ACI-0305666 and ACI-0352334.

solver has to be applied in order to deal with the high degree of nonlinearity and the nonsmooth blowup behavior in the system. One of the successful approaches to the numerical solution of the MHD system is based on the splitting of the system into two parts, where equations for the current and the vorticity are advanced in time, and the corresponding potentials are obtained by solving Poisson-like equations in a separate step. In such an explicit approach, to satisfy the CFL condition, the time step may become very small, especially in the case of fine meshes, and the Poisson solves must therefore be performed frequently. On the other hand, implicit time stepping presents an alternative approach that may allow the use of larger time steps. However, the non-smooth nature of the solution often results in convergence difficulties. In this work we take a fully coupled approach such that no operator splitting is applied to the system of MHD equations. More precisely, we first apply a third-order implicit time integration scheme, and then, to guarantee nonlinear consistency, we use a one-level Newton-Krylov-Schwarz algorithm to solve the large sparse nonlinear system of algebraic equations containing all physical variables at every time step. The focus of this paper is on the convergence and parallel performance studies of the proposed implicit algorithm.

2 Model MHD Problem

We consider a model MHD problem described as follows [2, 7]:

$$\left\{ \begin{array}{l} \nabla^2 \phi = U \\ \nabla^2 \psi = \frac{1}{d_e^2} (\psi - F) \\ \frac{\partial U}{\partial t} + [\phi, U] = \frac{1}{d_e^2} [F, \psi] + \nu \nabla^2 U \\ \frac{\partial F}{\partial t} + [\phi, F] = \rho_s^2 [U, \psi] + \eta \nabla^2 (\psi - \psi^0), \end{array} \right. \quad (1)$$

where U is the vorticity, F is the canonical momentum, ϕ and ψ are the stream functions for the vorticity and current density, respectively, ν is the plasma viscosity, η is the normalized resistivity, $d_e = c/\omega_{pe}$ is the inertial skin depth, and $\rho_s = \sqrt{T_e/T_i} \rho_i$ is the ion sound Larmor radius. The current density is obtained by $J = (F - \psi)/d_e^2$. The Poisson bracket is defined as: $[A, B] \equiv (\partial A/\partial x)(\partial B/\partial y) - (\partial A/\partial y)(\partial B/\partial x)$. Every variable in the system is assumed to be the sum of an equilibrium and a perturbation component; i.e. $\phi = \phi^0 + \phi^1$, $\psi = \psi^0 + \psi^1$, $U = U^0 + U^1$, and $F = F^0 + F^1$, where $\phi^0 = U^0 = 0$, $\psi^0 = \cos(x)$, and $F^0 = (1 + d_e^2) \cos(x)$ are the equilibrium components. After substitutions, we arrive at the following system for the perturbed variables:

$$\left\{ \begin{array}{l} \nabla^2 \phi^1 = U^1 \\ \nabla^2 \psi^1 = \frac{1}{d_e^2} (\psi^1 - F^1) \\ \frac{\partial U^1}{\partial t} + [\phi^1, U^1] = \frac{1}{d_e^2} [F^1, \psi^1] + \nu \nabla^2 U^1 + \frac{1}{d_e^2} \left(\frac{\partial \psi^1}{\partial y} F_{eqx} + \frac{\partial F^1}{\partial y} B_{eqy} \right) \\ \frac{\partial F^1}{\partial t} + [\phi^1, F^1] = \rho_s^2 [U^1, \psi^1] + \eta \nabla^2 \psi^1 + \left(\frac{\partial \phi^1}{\partial y} F_{eqx} + \rho_s^2 \frac{\partial U^1}{\partial y} B_{eqy} \right), \end{array} \right. \quad (2)$$

where $F_{eqx} = -(1 + d_e^2) \sin(x)$ and $B_{eqy} = \sin(x)$. The system is defined on a rectangular domain $\Omega \equiv [l_x, l_y] \equiv [2\pi, 4\pi]$, and doubly periodic boundary conditions are assumed. For initial conditions, we use a nonzero initial perturbation in ϕ^1 and a zero initial perturbation in ψ^1 . The exact form of the perturbation follows after some useful definitions. The aspect ratio is $\epsilon = l_x/l_y$. The perturbation's magnitude is scaled by $\delta = 10^{-4}$. We define $\tilde{d}_e = \max\{d_e, \rho_s\}$ and $\gamma = \epsilon \tilde{d}_e$. For the initial value of the ϕ perturbation we use

$$\phi^1(x, y, 0) = \begin{cases} \delta \frac{\gamma}{\epsilon} \operatorname{erf}\left(\frac{x}{\sqrt{2}\tilde{d}_e}\right) \sin(\epsilon y) & \text{if } 0 \leq x < \frac{\pi}{2} \\ -\delta \frac{\gamma}{\epsilon} \operatorname{erf}\left(\frac{x - \pi}{\sqrt{2}\tilde{d}_e}\right) \sin(\epsilon y) & \text{if } \frac{\pi}{2} \leq x < \frac{3\pi}{2} \\ \delta \frac{\gamma}{\epsilon} \operatorname{erf}\left(\frac{x - 2\pi}{\sqrt{2}\tilde{d}_e}\right) \sin(\epsilon y) & \text{if } \frac{3\pi}{2} \leq x \leq 2\pi. \end{cases} \quad (3)$$

Other quantities are set as: $U^1(x, y, 0) = \nabla^2 \phi^1(x, y, 0)$ and $F^1(x, y, 0) = \psi^1(x, y, 0) - d_e \nabla^2 \psi^1(x, y, 0)$. From now on, we drop the superscript and assume that the four fields ϕ , ψ , U and F represent the perturbed components only. In order to connect the stream functions to physical quantities the following definitions are used: $\mathbf{v} = e_z \times \nabla \phi$ and $\mathbf{B} = B_0 e_z + \nabla \psi \times e_z$. Here \mathbf{B} stands for the total magnetic field, B_0 is the guiding field in the z direction, and \mathbf{v} is the velocity in the plane perpendicular to the guiding field.

We discretize the system of PDEs with finite differences on a uniform mesh of sizes h_x and h_y in x and y directions, respectively. At time level t^k , we denote the grid values of the unknown functions $\phi(x, y, t)$, $\psi(x, y, t)$, $U(x, y, t)$, and $F(x, y, t)$, as $\phi_{i,j}^k$, $\psi_{i,j}^k$, $U_{i,j}^k$, and $F_{i,j}^k$. The time independent components of the system (2) are discretized with the standard second-order central difference method. For the time discretization, we use some multistep formulas, known as backward differentiation formulas (BDF) [8]. In this paper, we focus on a third-order temporal and second-order spatial discretizations as shown in (4), where $R_\phi^{k+1}(i, j)$, $R_\psi^{k+1}(i, j)$, $R_U^{k+1}(i, j)$, and $R_F^{k+1}(i, j)$ are the second-order accurate spatial discretizations of the time-independent components. We need to know solutions at time steps $k-2$, $k-1$ and k in order to compute a solution at time step $k+1$ in (4). Lower order schemes are employed at the beginning of the time integration for these start-up values.

$$\left\{ \begin{array}{l} R_\phi^{k+1}(i, j) = 0 \\ R_\psi^{k+1}(i, j) = 0 \\ \frac{h_x h_y}{6\Delta t} (11U_{i,j}^{k+1} - 18U_{i,j}^k + 9U_{i,j}^{k-1} - 2U_{i,j}^{k-2}) - R_U^{k+1}(i, j) = 0 \\ \frac{h_x h_y}{6\Delta t} (11F_{i,j}^{k+1} - 18F_{i,j}^k + 9F_{i,j}^{k-1} - 2F_{i,j}^{k-2}) - R_F^{k+1}(i, j) = 0 \end{array} \right. \quad (4)$$

3 One-level Newton-Krylov-Schwarz Method

At each time step, the discretized fully coupled system of equations (4) can be represented by $G(E) = 0$, where $E = \{\phi, \psi, U, F\}$. The unknowns are ordered mesh point by mesh point, and at each mesh point they are in the order ϕ, ψ, U , and F . The mesh points are ordered subdomain by subdomain for the purpose of parallel processing. The system is solved with a one-level Newton-Krylov-Schwarz (NKS), which is a general purpose parallel algorithm for solving systems of nonlinear algebraic equations. The Newton iteration is given as: $E_{k+1} = E_k - \lambda_k J(E_k)^{-1} G(E_k)$, $k = 0, 1, \dots$, where E_0 is a solution obtained at the previous time step, $J(E_k) = G'(E_k)$ is the Jacobian at E_k , and λ_k is the steplength determined by a linesearch procedure [4]. Due to doubly periodic boundary conditions, the Jacobian has a one-dimensional null-space that is removed by projecting out a constant. The accuracy of the Jacobian solve is determined by some $\eta_k \in [0, 1)$ and the condition $\|G(E_k) + J(E_k)s_k\| \leq \eta_k \|G(E_k)\|$. The overall algorithm can be described as follows:

1. Inexactly solve the linear system $J(E_k)s_k = -G(E_k)$ for s_k using a preconditioned GMRES(30) [11].
2. Perform a full Newton step with $\lambda_0 = 1$ in the direction s_k .
3. If the full Newton step is unacceptable, backtrack λ_0 using a backtracking procedure until a new λ is obtained that makes $E_+ = E_k + \lambda s_k$ an acceptable step.
4. Set $E_{k+1} = E_+$, go to step 1 unless a stopping condition has been met.

In step 1 above we use a right-preconditioned GMRES to solve the linear system; i.e., the vector s_k is obtained by approximately solving the linear system $J(E_k)M_k^{-1}(M_k s_k) = -G(E_k)$, where M_k^{-1} is a one-level additive Schwarz preconditioner. To formally define M_k^{-1} , we need to introduce a partition of Ω . We first partition the domain into non-overlapping substructures Ω_l , $l = 1, \dots, N$. In order to obtain an overlapping decomposition of the domain, we extend each subregion Ω_l to a larger region Ω'_l , i.e., $\Omega_l \subset \Omega'_l$. Only simple box decomposition is considered in this paper – all subdomains Ω_l and Ω'_l are rectangular and made up of integral numbers of fine mesh cells. The size of Ω_l is $H_x \times H_y$ and the size of Ω'_l is $H'_x \times H'_y$, where the H 's are chosen so that the overlap, $ovlp$, is uniform in the number of fine grid cells all around the perimeter, i.e., $ovlp = (H'_x - H_x)/2 = (H'_y - H_y)/2$ for every subdomain. The

boundary subdomains are also extended all around their perimeters because of the doubly periodic physical boundary. On each extended subdomain Ω'_l , we construct a subdomain preconditioner B_l , whose elements are $B_l^{i,j} = \{J_{ij}\}$, where the node indexed by (i, j) belongs to Ω'_l . The entry J_{ij} is calculated with finite differences $J_{ij} = 1/(2\delta)(G_i(E_j + \delta) - G_i(E_j - \delta))$, where $0 < \delta \ll 1$ is a constant. Homogeneous Dirichlet boundary conditions are used on the subdomain boundary $\partial\Omega'_l$. The additive Schwarz preconditioner can be written as

$$M_k^{-1} = (R_1)^T B_1^{-1} R_1 + \dots + (R_N)^T B_N^{-1} R_N. \quad (5)$$

Let n be the total number of mesh points and n'_l the total number of mesh points in Ω'_l . Then, R_l is an $n'_l \times n$ block matrix that is defined as: its 4×4 block element $(R_l)_{i,j}$ is an identity block if the integer indices $1 \leq i \leq n'_l$ and $1 \leq j \leq n$ belong to a mesh point in Ω'_l , or a block of zeros otherwise. The R_l serves as a restriction matrix because its multiplication by a block $n \times 1$ vector results in a smaller $n'_l \times 1$ block vector by dropping the components corresponding to mesh points outside Ω'_l . Various inexact additive Schwarz preconditioners can be constructed by replacing the matrices B_l in (5) with convenient and inexpensive to compute matrices, such as those obtained with incomplete and complete factorizations. In this paper we employ the LU factorization.

4 Numerical Results

To illustrate model behavior, we choose nominal values of the inertial skin depth $d_e = 0.08$ and the ion sound Larmor radius $\rho_s = 0.24$. The normalized resistivity and viscosity are chosen in the range $\eta, \nu \in [10^{-4}, 10^{-2}]$. Time in the system is normalized to the Alfvén time $\tau_A = \sqrt{4\pi n m_i l_x} / B_{y0}$, where B_{y0} is the characteristic magnitude of the equilibrium magnetic field and l_x is the macroscopic scale length [7]. Ω is uniformly partitioned into rectangular meshes up to 600×600 in size. The stopping conditions for the iterative processes are given as follows: relative reduction in nonlinear function norm $\|G(E_k)\| \leq 10^{-7} \|G(E_0)\|$, absolute tolerance in nonlinear function norm $\|G(E_k)\| \leq 10^{-7}$, relative reduction in linear residual norm $\|r_k\| \leq 10^{-10} \|r_0\|$, and absolute tolerance in linear residual norm $\|r_k\| \leq 10^{-7}$.

A typical solution is shown in Fig. 1. The initial perturbation in ϕ produces a feature-rich behavior in ψ , U , and F . The four variables in the system evolve at different rates: ϕ and ψ evolve at a slower rate than F and U . For $\eta = 10^{-3}$ and $\nu = 10^{-3}$ we observe an initial slow evolution of current density profiles up to time $100\tau_A$ and the solution blows up at time near $290\tau_A$. In the middle of the domain the notorious “X” structure is developed, as can be seen in the F contours, where the magnetic flux is reconnected. Similar reconnection areas are developed on the boundaries of the domain due to the periodicity of boundary conditions and the shape of the initial ϕ perturbation. In the reconnection regions sharp current density peaks (Fig. 2 (a)) are formed. We

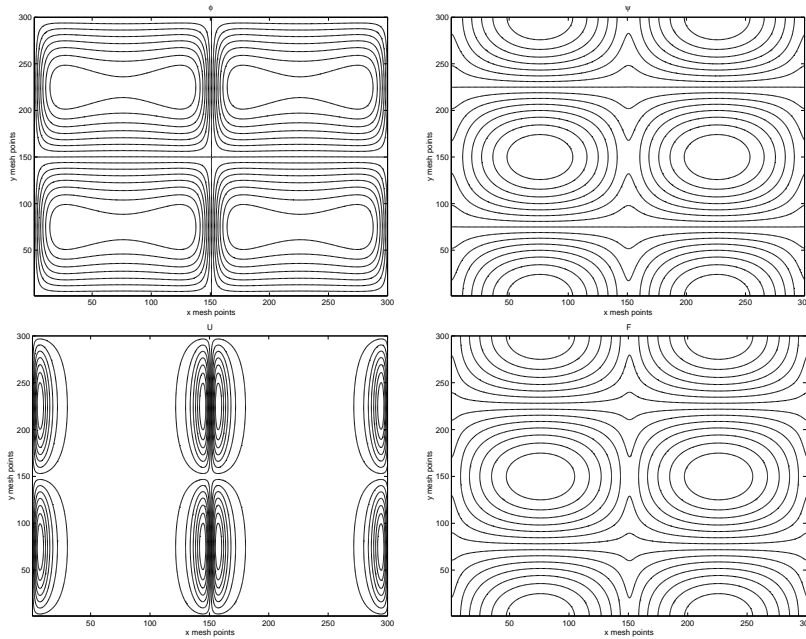


Fig. 1. Contour plots of ϕ (top left), ψ (top right), U (bottom left), and F (bottom right). The results are obtained on 300×300 mesh, $\Delta t = 1.0\tau_A$, $t = 100\tau_A$, $\eta = 10^{-3}$, $\nu = 10^{-3}$, implicit time stepping.

compare solutions obtained by our implicit method with these obtained with an explicit method [5]. Fig. 2 (b) shows that the third-order implicit method allows for much larger time steps and produces a solution that is very close to the solution obtained with the explicit algorithm, where the size of the time step is determined by the CFL constraint.

Next, we look at some of the machine dependent properties of the algorithm. Our main focus is on the scalability, which is an important quality in evaluating parallel algorithms. First, we look at the total computing time as a function of the number of subdomains and calculate $t(16)/t(np)$ which gives a ratio of time needed to solve the problem with sixteen processors to the time needed to solve the problem with np processors. Fig. 3 shows the results for a 600×600 mesh, and an overlap of 6 is used in all cases. We can see that the one-level algorithm scales reasonably well in terms of the compute time. Table 1 illustrates results obtained on a 600×600 mesh. The compute time scalability is attained despite the fact that the total number of linear iterations increases with the number of subdomains.

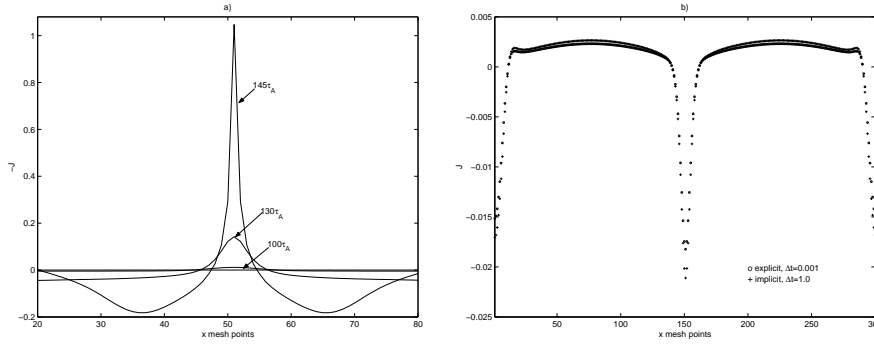


Fig. 2. a) Formation of current density peaks in the reconnection region, J , 100×100 mesh, $\eta = 10^{-2}$, $\nu = 10^{-2}$, $\Delta t = 1.0\tau_A$. b) Comparison plots of J obtained with the explicit method ($\Delta t = 0.001\tau_A$) and the implicit with $\Delta t = 1.0\tau_A$ at $t = 200\tau_A$ on 300×300 mesh with $\eta = 10^{-3}$ and $\nu = 10^{-3}$.

Table 1. Scalability with respect to the number of processors, 600×600 mesh. LU factorization for all subproblems, $ovlp = 6$. Time step $\Delta t = 1.0\tau_A$, 10 time steps, $t = 280\tau_A$. The problem is solved with 16 – 400 processors.

np	t [sec]	Total Nonlinear	Total Linear	Linear/Nonlinear
16	2894.8	30	1802	60.1
36	1038.1	30	2154	71.8
64	542.8	30	2348	78.3
100	340.5	30	2637	87.9
144	239.5	30	2941	98.0
225	167.8	30	3622	120.7
400	120.4	30	4792	159.7

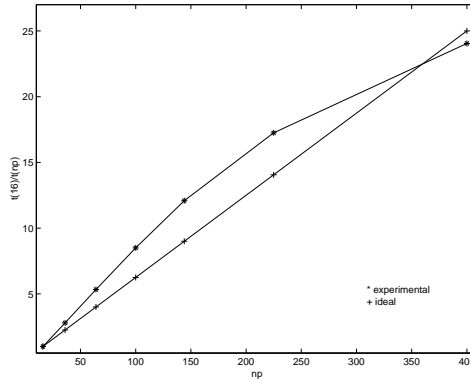


Fig. 3. Computing time scalability $t(16)/t(np)$, 600×600 mesh, $\eta = 10^{-3}$, $\nu = 10^{-3}$, $\Delta t = 1.0\tau_A$ with 16 – 400 processors, $t = 280\tau_A$. The data are collected over 10 time steps. The "*" shows experimental speedup values and "+" depicts the ideal speedup.

5 Conclusions and Future Work

The proposed fully coupled implicit scheme with a third-order temporal discretization allows much larger time steps than the explicit method, while still preserving the solution accuracy. One-level NKS converges well with the problem parameters in the specified range, given the right stopping conditions. Without a coarse space, the algorithm scales reasonably well for a large number of processors with a medium subdomain overlap. Future continuation of this work may include solutions of the MHD problem on finer meshes with a larger number of processors. Longer time integration with various η and ν values, as well as higher ρ_s to d_e ratios, may be helpful in the further understanding of the algorithm for the numerical solutions of MHD problems.

References

1. Balay S., Buschelman K., Eijkhout V., Gropp W.D., Kaushik D., Knepley M., McInnes L.C., Smith B.F., and Zhang H., *PETSc Users Manual*, ANL-95/11 - Revision 2.3.1, Argonne National Laboratory, (2006)
2. Cafaro E., Grasso D., Pegoraro F., Porcelli F., Saluzzi A., *Invariants and geometric structures in nonlinear Hamiltonian magnetic reconnection*, Phys. Rev. Lett., **80**(20), 4430–4433, (1998)
3. Chacon L., Knoll D.A., Finn J.M., *An implicit, nonlinear reduced resistive MHD solver*, J. Comput. Phys., **178**, 15–36, (2002)
4. Dennis J.E. and Schnabel R.B., *Numerical Methods for Unconstrained Optimization and Nonlinear Equations*, SIAM, Philadelphia, (1996)
5. Germaschewski K., *personal communications*
6. Goldston R.J., Rutherford P.H., *Introduction to Plasmas Physics*, IOP Publishing, (1995)
7. Grasso D., Pegoraro F., Porcelli F., Califano F., *Hamiltonian magnetic reconnection*, Plasma Phys. Control Fusion, **41**, 1497–1515, (1999)
8. Hairer E., Norsett S.P., and Wanner G., *Solving Ordinary Differential Equations I*, Springer-Verlag, (1991)
9. Ottaviani M., Porcelli F., *Nonlinear collisionless magnetic reconnection*, Phys. Rev. Lett., **71**(23), 3802–3805, (1993)
10. Ottaviani M., Porcelli F., *Fast nonlinear magnetic reconnection*, Phys. Plasmas, **2**(11), 4104–4117, (1995)
11. Saad Y., *Iterative Methods for Sparse Linear Systems*, SIAM (2003)
12. Strauss H.R., Longcope D.W., *An adaptive finite element method for magneto-hydrodynamics*, J. Comput. Phys., **147**, 318–336, (1998)